

9-21-1994

Characterization of Metal Aggregates by Scanning Microscopy: Particle Sizes and Space Distribution in Intermetallic Particles

M. O. Delcourt
Université Paris-Sud, France

F. Yala
Université Paris-Sud, France

E. Merlen
Institut Français du Pétrole, France

S. Remita
Université Paris-Sud, France

N. Keghouche
Université Paris-Sud, France

See next page for additional authors
Follow this and additional works at: <https://digitalcommons.usu.edu/microscopy>

 Part of the [Biology Commons](#)

Recommended Citation

Delcourt, M. O.; Yala, F.; Merlen, E.; Remita, S.; Keghouche, N.; and Delarue, E. (1994) "Characterization of Metal Aggregates by Scanning Microscopy: Particle Sizes and Space Distribution in Intermetallic Particles," *Scanning Microscopy*. Vol. 8 : No. 3 , Article 2.

Available at: <https://digitalcommons.usu.edu/microscopy/vol8/iss3/2>

This Article is brought to you for free and open access by the Western Dairy Center at DigitalCommons@USU. It has been accepted for inclusion in Scanning Microscopy by an authorized administrator of DigitalCommons@USU. For more information, please contact digitalcommons@usu.edu.



Characterization of Metal Aggregates by Scanning Microscopy: Particle Sizes and Space Distribution in Intermetallic Particles

Authors

M. O. Delcourt, F. Yala, E. Merlen, S. Remita, N. Keghouche, and E. Delarue

CHARACTERIZATION OF METAL AGGREGATES BY SCANNING MICROSCOPY: PARTICLE SIZES AND SPACE DISTRIBUTION IN INTERMETALLIC PARTICLES

M.O. Delcourt*, F. Yala, E. Merlen¹, S. Remita, N. Keghouche and E. Delarue

Laboratoire de Physico-Chimie des Rayonnements CNRS URA 75,
Bat 350, Université Paris-Sud, 91405 Orsay Cedex, France

¹Institut Français du Pétrole, 1 Avenue de Bois Préau, BP 311, 92506 Rueil Malmaison, France

(Received for publication March 26, 1994 and in revised form September 21, 1994)

Abstract

Various metal aggregates prepared using ionizing radiation were studied by microscopy techniques. A metal deposit onto a carbon felt obtained from solutions containing Pt and Ru was shown to consist of nanometric particles containing both metals. Another study deals with a subnanometric silver aggregate. The nuclearity of the aggregate was studied by scanning tunneling microscopy (STM). Additional information from pulse radiolysis experiments allowed the determination of the Ag_7^{3+} stoichiometry.

The third material consisted of Ag/Pd submicron powders (70/30 or 75/25 % w/w) used in electronics, and made of spherical bimetallic grains; X-ray diffraction showed segregation. The spatial distribution of each metal was obtained by combining space-resolved X-ray microanalysis in the transmission electron microscope, X-ray photoelectron spectroscopy and secondary ion mass spectrometry. Each grain was shown to be core/rind structured (core: pure Ag; rind: 10-15 nm thick 11 % Ag/89 % Pd w/w alloy).

Key Words: Metal aggregates, cluster, bimetallic, platinum, ruthenium, palladium, silver, catalysis, powder.

*Address for correspondence:

M. O. Delcourt
Laboratoire de Physico-Chimie des Rayonnements,
CNRS URA 75,
Bat 350,
Université Paris-Sud,
91405 Orsay Cedex,
France

Telephone number: +33-1-69 41 75 78
FAX number: +33-1-69 41 61 88

Introduction

A radiolytic process has been developed in our laboratory in order to obtain very small mono- or multi-metallic aggregates (Belloni and Delcourt, 1982; Delcourt, 1983; Belloni-Cofler *et al.*, 1984; Marignier *et al.*, 1985). In this process, highly reducing species, mainly solvated electrons, are generated by the radiation-solvent interaction in the case of polar solvents such as water. When metal ions are present in solution, they are reduced to the zero oxidation state and then the metal atoms, which are initially produced in their single solvated form, start coalescing. By different physical or chemical means (such as support, dispersing polymeric agent, or ligand) the aggregation process can be stopped at different times, so that a wide range of particle sizes is provided. When several metal ions are present in the initial solution, alloys can easily be synthesized by this process at room temperature. This paper shows how the scanning microscopy techniques combined in some cases with other techniques [pulse radiolysis, X-ray photoelectron spectroscopy (XPS), and secondary ions mass spectrometry (SIMS)] make it possible to determine the structure of some metal aggregates of very different sizes and compositions.

Extremely dispersed catalytic deposits are required for use in electrodes for fuel cells. Indeed, the catalysts are made of precious metals, mainly Pt; for these fuel cells to be economically feasible, it must be possible to place almost every working atom at the surface of the particles: only the nanometric scale meets with this objective. These nanometric particles must be deposited onto a conductive material. Furthermore, in many cases, Pt-based alloys would be more suitable than pure Pt, especially in order to prevent poisoning of the catalyst. As a first example, Pt/Ru deposits on carbon felts are investigated.

In the last years, there has been increasing interest in metal oligomer aggregates either isolated in the gas phase or trapped inside a solid matrix, or in liquid solution, due to important size effects appearing for low aggregation numbers (Berry, 1993). Stabilization of

several oligomer silver aggregates has been achieved recently through irradiation of Ag^+ solutions in the presence of polyacrylate $[-\text{CH}_2-\text{CH}(\text{COO}^-)]_p$ (Mostafavi *et al.*, 1990a,b, 1993). They have been characterized by their optical spectra, and have been assigned to $(\text{Ag}_{m+n})^{m+}$ species, with approximate n values ≤ 12 . One of these oligomer clusters, denoted Ag_a (ultra violet, UV, band at 290 nm, blue colored) is the first example of such a small aggregate stabilized for so long in solution: it can be kept for years, thus providing the opportunity to study its physical and chemical properties. From recent pulse radiolysis experiments, the number of neutral silver atoms (n) in this cluster has been found to be 4, as deduced from the number of kinetic steps during the growth process (Mostafavi *et al.*, 1992). We describe here how scanning tunneling microscopy (STM) has been used to obtain the overall nuclearity $n + m$ (Remita *et al.*, 1994).

Intermetallic Ag/Pd powders are in increasing demand by the electronics industry (Pepin, 1991), where they are used in multilayer ceramic chip capacitors to make thin conductive electrode films and termination inks. A point of major interest regarding these powders is the distribution of the metals in the submicron particles of the powder. Only a true intermetallic character, i.e., the presence of both metals in each particle, as either fully alloyed or segregated in very small domains, can guarantee the required performance (high conductivity, low thickness) for low-cost electrodes. We report here measurements performed on powders recently synthesized at CLAL (Paris, France) by a new process producing spherical grains with a low size dispersion, at about 0.3 μm in diameter, and containing Ag/Pd 75/25 and 70/30% w/w (Delarue *et al.*, 1995).

Materials and Methods

The chemicals used were pure grade reagents: K_2PtCl_4 , RuCl_3 , AgNO_3 and Pd nitrate from CLAL, Ag_2SO_4 from Fluka (St. Louis, MO, USA), 2-propanol from Merck (Darmstadt, Germany), polyacrylic acid from Aldrich (St. Louis, MO; as aqueous solution 50% w/w, molecular weight, MW = 5000), NaOH, HNO_3 and $\text{K}_2\text{Cr}_2\text{O}_7$ from Prolabo (Paris, France), CO_2 from Air Liquide (St. Andre, France). The irradiations were carried out with a ^{60}Co gamma source (dose rate: 0.5 $\text{Mrad}\cdot\text{h}^{-1}$, i.e., 5 $\text{kGy}\cdot\text{h}^{-1}$).

Platinum-ruthenium

The carbon felts (RVG 2000 from Carbone-Lorraine, Amiens, France) were cut out as 5 x 5 cm^2 samples, pretreated as described below, rinsed with water, and then immersed into an aqueous solution containing 0.2 $\text{mol}\cdot\text{l}^{-1}$ 2-propanol, 10^{-3} $\text{mol}\cdot\text{l}^{-1}$ K_2PtCl_4 and 3 x

10^{-4} $\text{mol}\cdot\text{l}^{-1}$ RuCl_3 . After 24 hours, the sample was deaerated by nitrogen bubbling and subsequently irradiated with 1 Mrad. After irradiation, the sample was rinsed with water, sonicated, and finally dried. The microscopic observations were carried out on a JEOL (Croissy-sur-Seine, France) 2010 transmission electron microscope (TEM) and on a VG (Fisons Instruments, Arcueil, France) HB5 scanning transmission electron microscope (STEM), the latter equipped with a Tracor (Fisons) 524 [with a Kevex (Fondis, Guyancourt, France) Si(Li) diode] energy dispersive X-ray analyzer (X-EDS). The observed X-rays for quantitative analysis were L_{α} for Pt (at 9.44 keV) and Ru (at 2.56 keV).

Silver aggregates

The aqueous solutions containing 10^{-3} $\text{mol}\cdot\text{l}^{-1}$ Ag_2SO_4 , 0.2 $\text{mol}\cdot\text{l}^{-1}$ polyacrylic acid and 0.2 $\text{mol}\cdot\text{l}^{-1}$ 2-propanol were adjusted to a pH of 10.6 by NaOH. Deaeration and irradiation were carried out as above (dose: 100 krad, providing only partial reduction). STM observation was carried out in air at atmospheric pressure, with a Nanoscope III (Digital Instruments, Santa Barbara, CA) conveniently suspended for vibration isolation. Highly oriented pyrolytic graphite (HOPG, Union Carbide ZYH monochromator) was employed as a substrate. The tip quality was checked by imaging bare freshly cleaved HOPG with atomic resolution. All images were obtained in constant tunneling current mode. The deposition of the silver clusters from the solution was carried out in freshly cleaved HOPG. A droplet of the solution (a few microlitres) was put on the substrate surface, then most of the liquid was removed by capillarity with a residue-free paper (Joseph type). Finally, the sample was dried at 80°C for 10 minutes in an oven.

Silver palladium powder

X-ray diffraction was carried out on a Philips diffractometer equipped with a PW-1720 X-ray source (Cu K_{α}) and a PM-8203 recorder. Silver, palladium and their alloys are known to give face-centered cubic (fcc) crystals. According to Vegard's law, the composition of an Ag/Pd alloy can be deduced from the position of the diffraction peaks. The microscopic observations were carried out in a JEOL 2000 EX TEM equipped with a X-ray microanalysis spectrometer (Tracor Northern series 2) with a Li-doped silicon diode providing 149 eV resolution. XPS was carried out on a Leybold Heraeus (Köln, Germany) spectrometer, and SIMS on a IMS 3f CAMECA (Courbevoie, France) apparatus, the incident beam consisting of $^{133}\text{Cs}^+$ ions accelerated by 10 kV. For XPS and SIMS measurements, the samples were prepared as follows: a small quantity of powder was gently pressed (30 bars) on a tin disk so that the grains

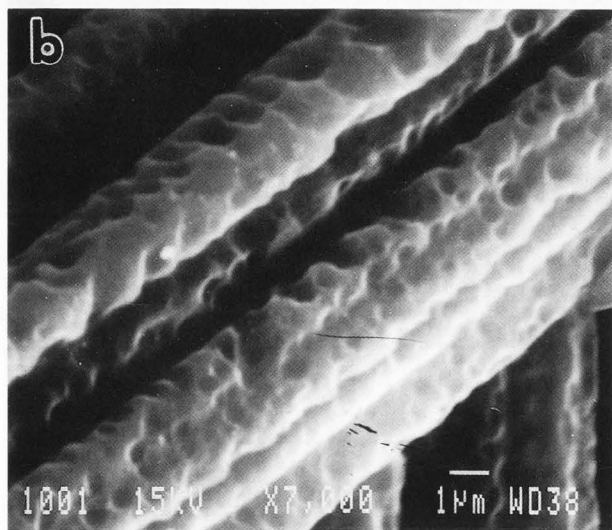
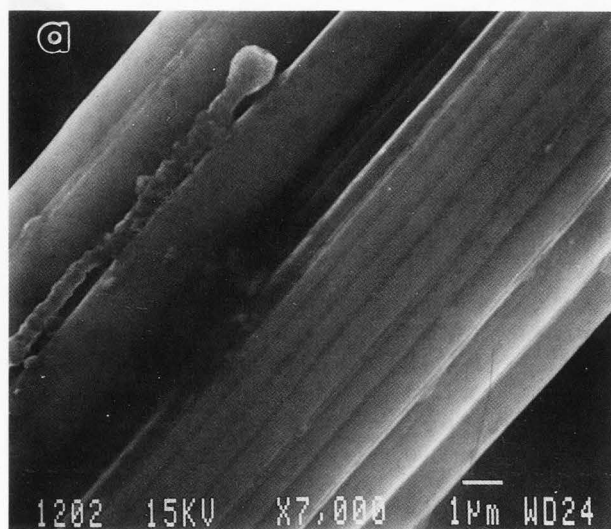


Figure 1. Scanning electron micrographs of the carbon substrate before (a) and after (b) thermal pretreatment (950°C under CO₂ flow). Bars = 1 µm.

were inserted into the tin matrix without being significantly distorted. Thus, in the first layer, the spherical particles were tangential to the external plane (scheme as shown later in Figure 7).

Results and Discussion

Bimetallic character of nanometric Pt/Ru particles on a carbon surface

The radiolytic process was used in order to prepare nanometric mono and bimetallic deposits on carbon felts. In order to increase the surface area and to functionalize the support (by creation of surface oxidized groups, e.g., carboxylate) so as to improve the metal ion

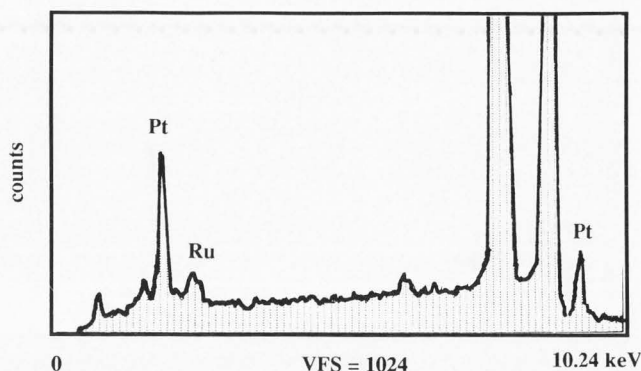


Figure 2. X-ray microanalysis spectrum for a single particle.

impregnation and the carbon-metal interaction, several pretreatments have been tried (Keghouche, 1993) among which electrochemical treatment in HCl or H₂SO₄, exposure to NaOCl or HNO₃ or/and K₂Cr₂O₇, and electrochemical/ chemical combinations. Thermal treatment at 930°C under CO₂ flow appears to be most efficient until 10% mass loss is reached. After this treatment, the initially smooth carbon fibers become rough as shown by SEM (Figure 1). The impregnation of K₂PtCl₄ aqueous solutions is faster than that of H₂PtCl₆ although still rather slow (about 0.1 mg/cm² per day). The adsorption of PtCl₄²⁻ ions was followed by UV absorption spectrophotometry: the solution became transparent, which indicated complete fixation of these ions. Therefore, during the reduction step, the radiolytic species (solvated electrons, radicals) produced in the liquid phase operate at the solid/liquid interface where the Pt ions are fixed. In this way, the Pt/support interaction is maximized, thus minimizing the Pt/Pt interaction responsible for the growth of particle. Under these conditions, after reduction, the deposits appear as 2 nm-sized particles homogeneously dispersed at the surface (TEM and STEM observation) for low Pt loadings (0.2 mg Pt.cm⁻² of geometric electrode). The limiting factor has been found to be the relatively low specific surface area of the carbon material. Work is now in progress with high surface carbon powders which can be highly loaded (17% w/w Pt) in the same way without loss of their dispersive power.

It is known that in electro-oxidation of methanol, a candidate for fuel cells, Pt electrodes can get poisoned (Lamy and Léger, 1991). Ru has been added in order to prevent poisoning. Aqueous solutions containing both K₂PtCl₄ and RuCl₃ were impregnated onto a carbon felt and subsequently radiolytically reduced. The initial atomic ratio was Pt/Ru 75/25%. The particle size, as analyzed by STEM, was found to be 1 to 4 nm as for

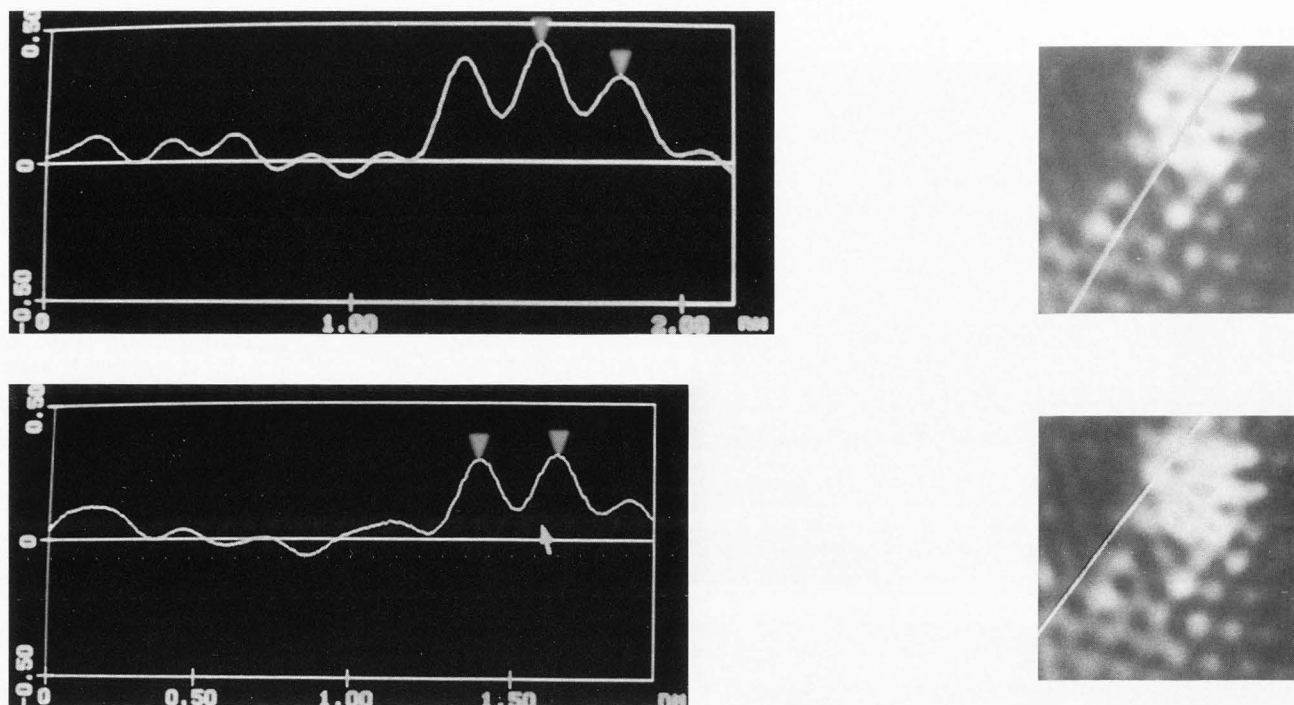


Figure 3. Scanning tunneling microscope images (in air) of a silver oligomer on HOPG, with section analysis according to two different axes. (a). 3 atoms are observed with an interatomic distance of 0.242 nm; (b). 2 atoms are observed with an interatomic distance of 0.249 nm.

Table 1. X-ray microanalysis of a radiolytic Pt/Ru deposit.

Site type	Analyzed area nm ²	Magnification	Pt at. %	Ru at. %
single particle	8 x 6	5 x 10 ⁶	67	33
single particle	8 x 6	5 x 10 ⁶	68	32
single particle	8 x 6	5 x 10 ⁶	58	42
single particle	4 x 3	10 ⁷	64	36
naked support	8 x 6	5 x 10 ⁶	43	57
naked support	40 x 30	10 ⁶	55	45
cluster	20 x 15	2 x 10 ⁶	73	27
cluster	20 x 15	2 x 10 ⁶	73	27
cluster	20 x 15	2 x 10 ⁶	81	19
cluster	20 x 15	2 x 10 ⁶	79	21
particles + support	80 x 60	5 x 10 ⁵	51	49

pure Pt. Diffraction attempts were unsuccessful due to the small quantity of material. In order to analyze the spatial distribution of both metals, X-ray microanalysis was performed by focusing the electron beam on very small areas (down to 4 x 3 nm²): such a high resolution makes it possible to analyze single particles as well as clusters of a few particles, and areas of the support where no particle could be detected. In Table 1, typical

results thus obtained are displayed, while Figure 2 shows an example of an X-ray spectrum with the beam focused on a single particle. In any position, both Pt and Ru were detected, even at sites where no particle was observed.

The results in Table 1 show the bimetallic character of the deposit in any place. The Pt/Ru ratio was dependent on the observed site and can be summarized as follows: about 50 Pt/50 Ru atomic % for the support without any observable particle; 76/24% for clusters consisting of a few particles; and 63/37% for single particles.

In reality, the analysis always includes a contribution of the support because the electron beam goes through the sample: consequently the Ru content, which is higher on the support, is always overestimated when particles are observed, and this is all the more true when they are isolated. Therefore, we conclude that the clusters give the best estimation of the composition of the observable particles, which reveals them to be very close to the initial mixture. The presence of both Pt and Ru on the support in places where no particle is detectable indicates that either particles under the detection threshold (ca. 1 nm under the conditions used) are dispersed all over the support surface, or that there are some remaining unreduced metal ions. Since Pt is always very

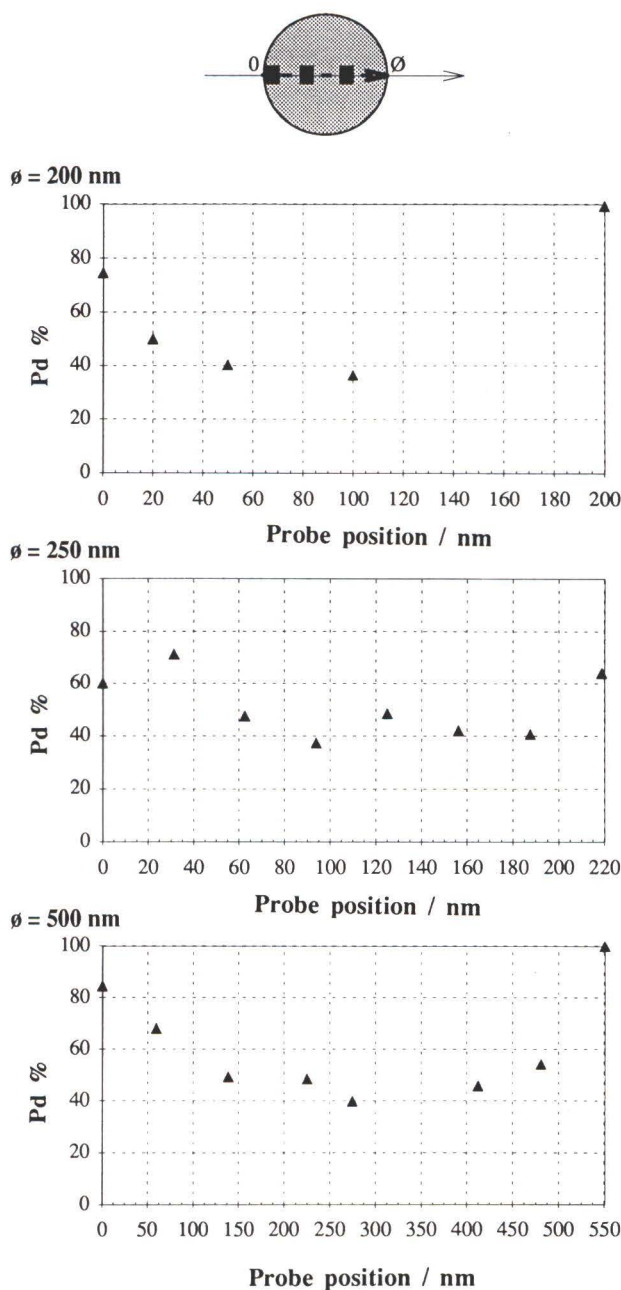


Figure 4. Composition changes along a diameter in single grains of a 75% Ag/25% Pd powder. The probe position is set as shown in the upper scheme.

easily reduced under radiation, the first hypothesis seems more likely.

Determination of the stoichiometry of a subnanometer silver aggregate (oligomer cluster)

In many places on the HOPG surface, STM observation was not possible due to the presence of the non-conducting polymer. However, in some areas, oligo-

mers were observed, especially in the middle of the flat HOPG terraces. They were either isolated or formed groups without special arrangements. A typical single oligomer is shown in Figure 3: a well defined area corresponding to the cluster is observed over the hexagonal structure of graphite, which is clearly resolved at the atomic level. The section analysis in Figure 3a shows the presence of three atoms along the diameter. When analyzing along another axis (Figure 3b), only two atoms were detected. The sharpness of such images indicates the absence of perturbations induced by polymer anions which would give rise to much larger features. Such single particles, which are well representative of the observed clusters, appear as hexagons with a diameter of about 0.7 nm, and a mean height of about 0.3-0.4 nm. From the STM images, it appears that the silver cluster is made of 7 silver atoms located at the same height over the substrate surface. In some cases, a single signal of greater height is observed which may be an additional silver atom on the top of the cluster or an exalted effect of the tunneling current due to a peculiar arrangement of the atoms in the clusters, so that a nuclearity of 8 cannot be excluded. Ag-Ag distances have been measured in sections along different axes (see Figure 3a and 3b). Values between 0.242 and 0.256 nm have been obtained.

A total number $n + m = 7$ (or possibly 8) and $n = 4$ leads to the value $m = 3$ (or 4) for the number of charges in the $(Ag_{m+n})^{m+}$ cluster. The clusters observed by STM are likely to be the result of complete reduction of these $(Ag_{4+m})^{m+}$ precursors. This would also explain the absence of the stabilizing polyanion in the vicinity of the resulting fully reduced clusters: indeed polyacrylate has been shown to interact through coulombic attraction between the negative anion groups and the positive excess silver charges (Mostafavi *et al.*, 1993). The observed hexagonal shape suggests the possibility of flattening of the silver clusters as a consequence of adsorption and/or thermal treatment: their structure in solution is likely to be more spherical.

Space resolved structure of submicron grains of an intermetallic Ag/Pd powder

X-ray diffraction provided two series of peaks: one consisted of well-defined narrow peaks whose positions coincide with those expected for pure silver; the other was made up of less intense broader peaks close to those of pure palladium. Therefore, the powders clearly appear to contain two distinct phases: only a weak alloying is observed for the Pd phase. At this point of the study, two models are possible: either a mixture of monophasic particles, silver grains and palladium grains, each one being pure or almost pure metal; or a powder of bimetallic particles with internal segregation in two phases.

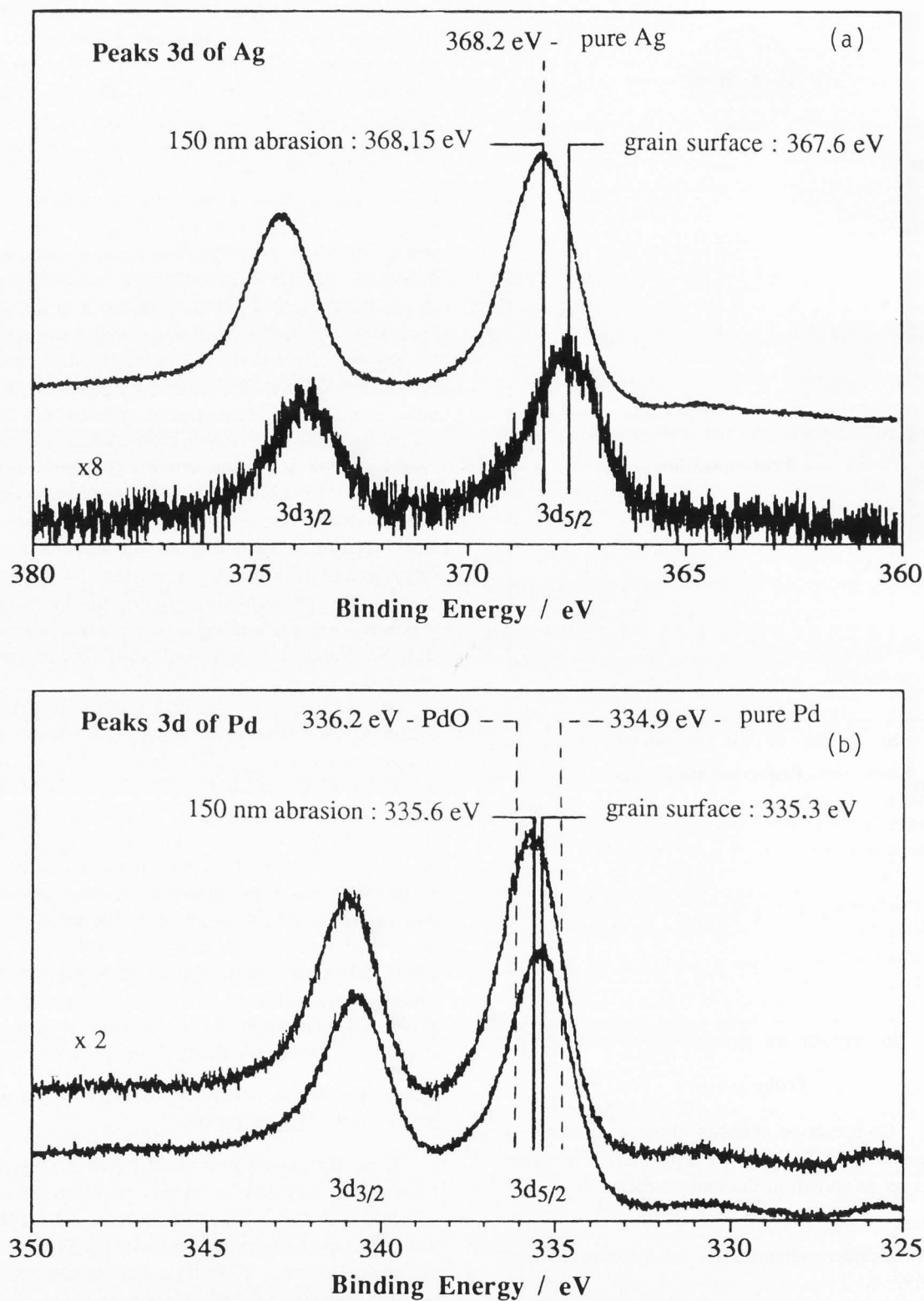


Figure 5. XPS peaks ($3d_{3/2}$ and $3d_{5/2}$) for Ag and Pd at the beginning of the run (a, top) and after 150 nm (b, bottom) abrasion. For calibration, the positions of Ag ($3d_{5/2}$) and Pd ($3d_{5/2}$) for pure metals and PdO are marked in dashed lines.

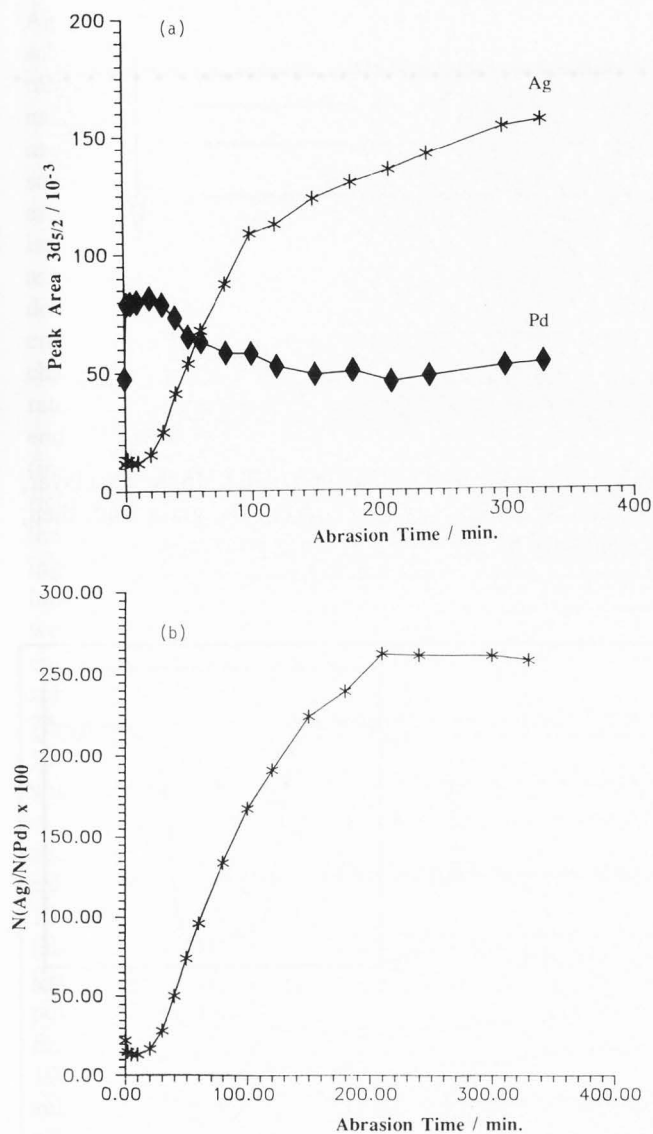


Figure 6. Changes in the Ag/Pd ratio with the abrasion time (Argon abrasion rate: $0.5 \text{ nm} \cdot \text{min}^{-1}$). (a) Peak area for each metal. (b) Relative abundance corrected for cross-sections.

Diffraction on a single particle has been achieved in the TEM, and also gives the two series of peaks as described above, which indicates a bimetallic character.

In order to determine the space arrangement of Ag and Pd in the particles, three different methods were used. First, X-ray microanalysis in the TEM was performed. The size of the probe ($15 \text{ nm} \times 15 \text{ nm}$) is noticeably smaller than the particle size (300 nm) thus allowing a space-resolved analysis of a single particle. Such an analysis was carried out on 20 different particles. The probe was moved along a diameter of the particle as shown in Figure 4 (upper scheme). The Pd percentage was measured as a function of the probe posi-

tion: in every case, the Pd content was found to decrease when the beam was moved from the edge to the central region, and then to increase again from the centre to the other edge. The fact that the Pd content found at any point was relatively high (about 40%), higher than the mean content, can be explained in two ways: first, the incident electron beam must always cross the surface layer which is Pd-rich; second, the spectrometer is adapted to thin planar samples so that, in spite of corrections for absorption and secondary emission, the surface layer is always overestimated.

The second method is XPS which allows a quantitative surface analysis of the elements through the number of electrons extracted from 3d levels of both Ag and Pd atoms. A progressive abrasion of the surface layer is carried out with an Ar^+ ion beam ($0.5 \text{ nm} \cdot \text{min}^{-1}$) so that the depth-composition profile can be determined. The results are shown in Figure 5. Ag and Pd signals were both observed at any time with relative intensities changing with depth. Figure 6 shows that a plateau value is reached after 200 minutes i.e., 100 nm. The initial surface layer appears to be very Pd-rich (Pd/Ag = 89/11% after correction for the respective cross-sections 9.54 and 10.68). After 10 nm, a progressive enrichment in silver is observed up to the particle core (mean particle diameter: 300 nm), thus confirming the model of a silver core surrounded by a Pd-rich alloyed layer ca. 10-15 nm thick. At greater depth (100-200 nm, i.e., 200-400 minutes), the ratio Ag/Pd is found to be 72/28%, close to the mean ratio (75/25): at this depth, the analyzed layer is randomized due to the size distribution of the powder particles (Figure 7). More detailed information can be deduced from the peak positions: both Ag and Pd peaks are shifted to higher energies with increasing depth, with a more marked effect for Ag. After 150 nm abrasion, which is the mean position of the centers of the first particle layer, the Ag $3d_{5/2}$ peak (Figure 5) is exactly at the energy of pure silver which is very well known since it is commonly used for calibration: the Ag shift is a chemical shift due to the progressive change from a surface alloy (with a low Ag content) to a pure silver core. The shift of the Pd peak, hardly significant, might correspond to a Pd gradient with increasing values for positions close to the particle surface. PdO was not observed since the corresponding shift would be on the opposite side. However, some oxygen was detected, but quantitative estimation was not possible.

Finally, the third method, SIMS, can provide comparable depth-profiled composition of the powder grains. The incident $^{133}\text{Cs}^+$ beam continuously hits the sample surface: CsM^+ ions (where M is a metal atom taken out of the surface) are formed and the mass of these ions is analyzed. The beam progressively erodes the sample, thus forming a hole. Due to the close atomic weights of

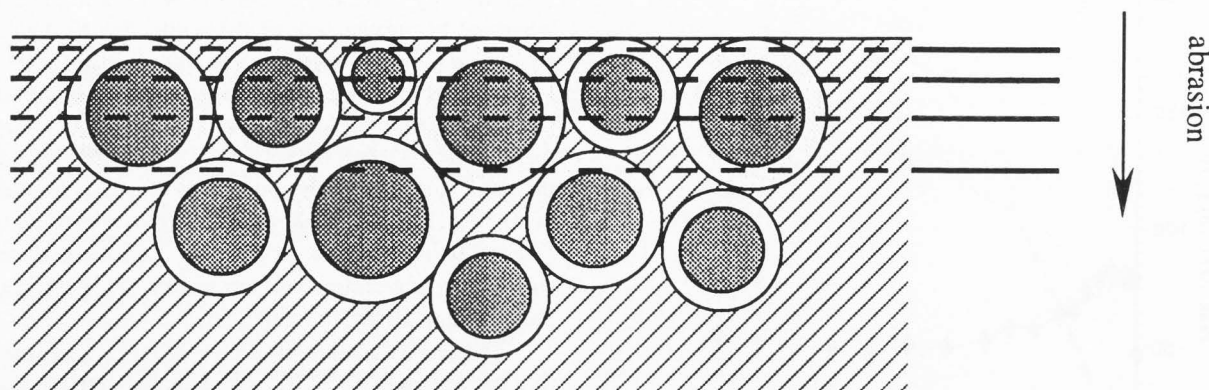


Figure 7. Scheme showing the arrangement of the powder grain in a sample pressed into a tin pellet. In the first layer, the grains are tangential to the sample surface so that the XPS and SIMS analysis first concern the grain rind; then, when abrasion goes on, the probe position is more and more randomized.

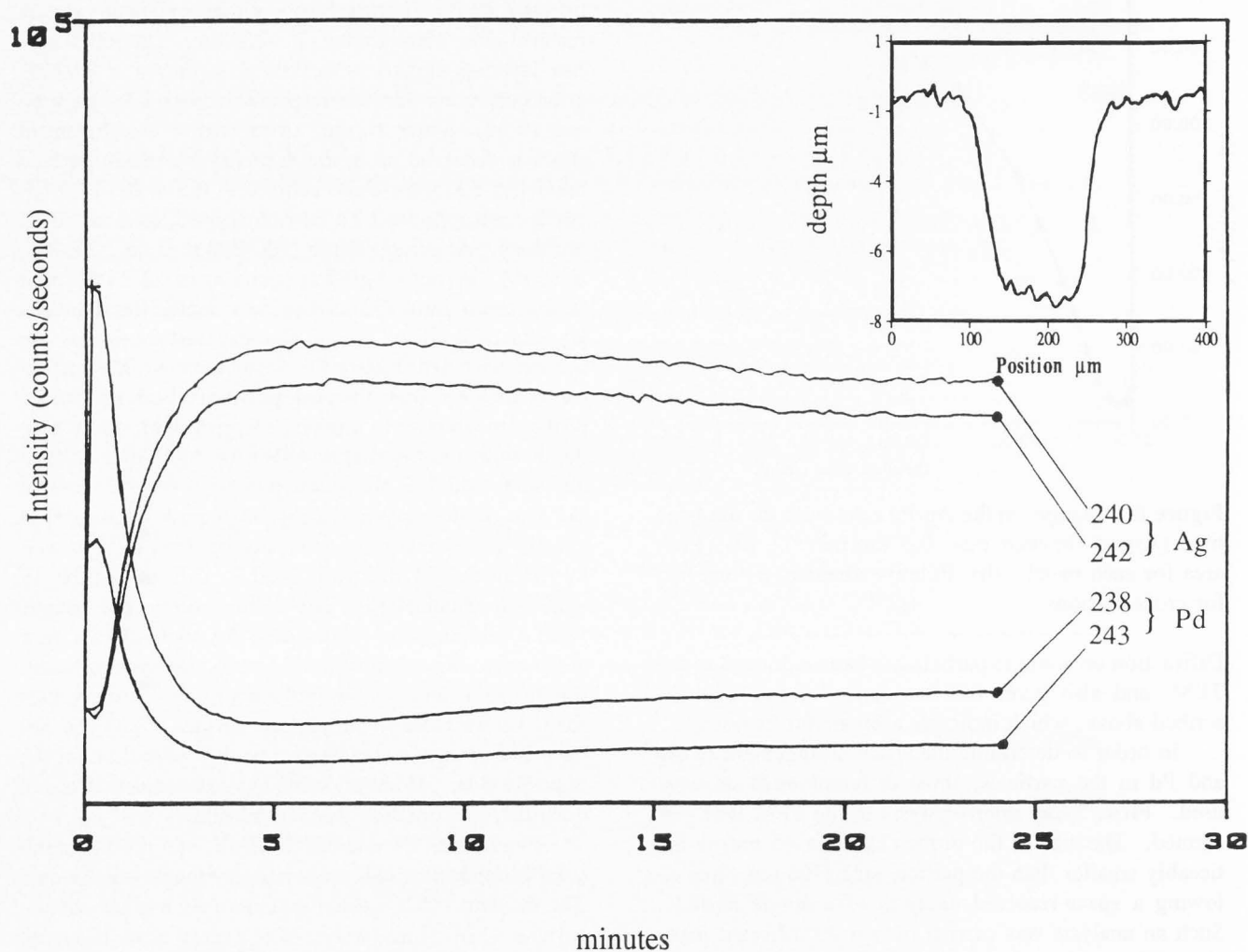


Figure 8. Changes in the ion beam intensity measured by SIMS for a few relevant masses with erosion time. **Insert:** Crater profile measured with a profilometer.

Ag and Pd, absolute identification of the peaks is achieved by comparing their intensities with the natural relative abundances of Ag and Pd isotopes. A weak signal is obtained for PdHCs⁺ which can be quantitatively neglected. In Figure 8, the intensities measured for some significant masses are shown as a function of the erosion time. The 238 and 243 masses correspond to Pd isotopes ¹⁰⁵Pd and ¹¹⁰Pd; the peaks at 240 and 242 are assigned to ¹⁰⁷Ag and ¹⁰⁹Ag. The measured intensities do not allow quantitative measurements because the cross-sections are not known for this material. Only the changes with time (or depth) are significant: the erosion rate (20 nm.min⁻¹) is deduced from the hole depth at the end of the experiment, as measured by a profilometer (inset Figure 8). The results show that: the surface is richer in Pd than the core; and some Ag is present from the beginning, i.e., at the particle surface, thus confirming the core/rind model. After 20 nm erosion, no oscillations are found as would be expected if the particles were exactly monodisperse: almost constant signals then correspond to the mean composition of the actual spheres (Figure 7). From the known value Ag/Pd = 75/25% of this mean composition, the approximate ratio 12/88% is derived for the surface layer, in agreement with the results given above.

All three techniques provide converging information about the structure of the powder particles. Each spherical grain is made of a pure silver core surrounded by a 10-15 nm thick alloyed layer with a high Pd content (about 89%), possibly even higher, closer to the surface. Let us note that in spite of its biphasic structure, this powder results in conducting layers with excellent performance [16 mΩ.cm for 2 μm thickness (Yala *et al.*, 1995)] due to the presence of both metals inside each submicron grain, so that interdiffusion rapidly occurs when the layer is heated.

In conclusion, it has been shown that different scanning microscopy techniques can be successfully used in solving important practical problems: the bimetallic character of the Pt/Ru deposits is a key point for application in fuel cells. STM allowed the determination of the stoichiometry of Ag₇³⁺ clusters, too small for detection by electron microscopy. Finally, the space-resolved structure of a Ag/Pd powder grain shows how three analytical techniques can be combined to provide unambiguous information, namely about the core/rind structure of the grain and the local composition of each domain.

Acknowledgements

This work was supported by the European Community (JOUE 0037-C program) and ADEME. The authors thank J. Feliu (University of Alicante, Spain), C. Séverac and C. Haut (Laboratoire de Métallurgie Phy-

sique, Orsay, France) and C. Grattapain (Laboratoire de Physique des Solides de Bellevue, Meudon, France) for giving them access to their techniques and for helpful discussions. They also thank CLAL for providing the precious metal salts and the Ag/Pd powder.

References

- Belloni J, Delcourt MO (1982) Radiation induced preparation of metal catalysts: Iridium aggregates. *New J. Chem.* **6**, 507-509.
- Belloni-Cofler J, Marignier JL, Delcourt-Euverte MO, Minana-Lourseau M (1984) Non-noble metal catalytic microaggregates, a method for their preparation and their application in the catalysis of the photoreduction of water. CNRS French patent number 8409196 (1984); European patent number 85.401154.11 (1985); US patent number 2,629,709 (1986).
- Berry RS (1993) (ed.). *Small Particles and Inorganic Clusters*. Proceedings of the International Meeting on Small Particles and Inorganic Clusters. Chicago (USA), Sept. 1992. *Z. Phys. D Atoms, Molecules and Clusters*. Supplement to vol. 26.
- Delarue E, Mostafavi M, Delcourt MO, Regnault D (1995) Silver-Palladium submicronic powders: part I. Morphology and Thermal Properties. *J. Mater. Sci.* In press.
- Delcourt MO, Keghouche N, Belloni J (1983) Radiation reduced Platinum sols: characterization and catalytic efficiency. *New J. Chem.* **7**, 131-136.
- Keghouche N (1993) *Agrégats métalliques et clusters oligomères élaborés par voie radiolytique* (Metal aggregates and oligomeric clusters prepared by radiolysis). Ph.D. Thesis. Univ. Constantine (Algeria).
- Lamy C, Léger JM (1991) Electrocatalytic oxidation of small organic molecules at platinum single crystals. *J. Chim. Phys.* **88**, 1649-1671.
- Marignier JL, Belloni J, Delcourt MO, Chevalier JP (1985) Microaggregates of non-noble metals and bimetallic alloys prepared by radiation-induced reduction. *Nature* **317**, 344-345.
- Mostafavi M, Keghouche N, Delcourt MO, Belloni J (1990a) Ultra-slow aggregation process for silver clusters of a few atoms in solution. *Chem. Phys. Lett.* **167**, 193-197.
- Mostafavi M, Keghouche N, Delcourt MO (1990b) Complexation of silver clusters of a few atoms by a polyanion in aqueous solution: pH effect correlated to structural changes. *Chem. Phys. Lett.* **169**, 81-84.
- Mostafavi M, Delcourt MO, Keghouche N, Picq G (1992) Early steps of formation of silver/polyacrylate complexed clusters. A pulse radiolysis study. *Radiat. Phys. Chem.* **40**, 445-450.
- Mostafavi M, Delcourt MO, Picq G (1993) Study of

the interaction between polyacrylate and silver oligomer clusters. *Radiat. Phys. Chem.* **41**, 453-459.

Pepin JG (1991) Multilayer ceramic capacitor electrodes: powder technology and fired properties. *J. Mater.: Electron.* **2**, 34-39.

Remita S, Orts JM, Feliu JM, Mostafavi M, Delcourt MO (1994) STM identification of silver oligomer clusters prepared by radiolysis in aqueous solution. *Chem. Phys. Lett.* **218**, 115-121.

Yala F, Delarue E, Delcourt MO, Haut C, Severac C, Grattapain C (1995) Silver-palladium submicronic powders: part II. Structural Characterization. *J. Mater. Sci.* In press.

Discussion with Reviewers

C.E. Bamberger: How does or would the action of chemical reductants (H_2 , $NaBH_4$) compare with radiation for the low Pt loadings used?

R. Natesh: In the experiments, 1 Mrad and 100 krad, respectively, were used to reduce the starting reagents. What are the advantages of using radiation, instead of chemical means, to reduce these compounds (in terms of reaction speed, final products obtained, chemical contamination, etc.)?

Authors: Comparable Pt deposits can be obtained by using H_2 reductant as long as the loadings are low. Radiolysis is a powerful method to increase the Pt loading and to make alloys; the advantages of the radiolytic process are described in Belloni *et al.* (1982, 1984). There is no contamination problem since there is no contact between the sample and the radioactive elements, and the energy of the radiation (1.3 MeV) is not enough to induce nuclear reactions.

C.E. Bamberger: Why would the support be richer in Ru? Could it be related to a significant difference in the diffusion of the Pt- and Ru-containing species which may result from hydrolysis? Since no pH measurement is given, estimation of the species cannot be done.

Authors: We do not have any explanation of the higher Ru content on the support. Under the conditions used, the hydrolysis of Ru is not important.

R. Natesh: What are the advantages of using HOPG as a substrate? Does the hexagonal structure influence the oligomers also to be precipitated in a hexagonal shape (Figure 3)? Will the arrangements of the silver aggregates change, if a different material with a different crystal structure is used as a substrate?

Authors: There is good compatibility between HOPG and silver distances. Possibly the image would be modified by changing the substrate.